Available online at www.sciencedirect.com
ScienceDirect
Journal of Solid State Chemistry 179 (2006) 3709–3717
JOURNAL OF SOLID STATE CHEMISTRY
www.elsevier.com/locate/jssc

Synthesis, structure, magnetic susceptibility and Mössbauer and Raman spectroscopies of the new oxyphosphate $Fe_{0.50}TiO(PO_4)$

S. Benmokhtar[a,*], A. El Jazouli[a], J.P. Chaminade[b], P. Gravereau[b], A. Wattiaux[b], L. Fournès[b], J.C. Grenier[b], D. Waal[c]

[a]*LCMS, UFR Sciences des Matériaux Solides, Faculté des Sciences Ben M'Sik, Casablanca, Morocco*
[b]*Institut de chimie de la matière condensée de Bordeaux (ICMCB-CNRS), 87, av. du Dr. A. Schweittzer-33608 Pessac, France*
[c]*Department of Chemistry, University of Pretoria, 0002 Pretoria, South Africa*

Received 22 June 2006; received in revised form 4 August 2006; accepted 5 August 2006
Available online 11 August 2006

Abstract

A new iron titanyl oxyphosphate $Fe_{0.50}TiO(PO_4)$ was synthesized by both solid-state reaction and Cu^{2+}–Fe^{2+} ion exchange method. The material was then characterized by X-ray diffraction, Mössbauer spectroscopy, magnetic susceptibility measurements and Raman spectroscopy. The crystal structure of the compound was refined, using X-ray powder diffraction data, by Rietveld profile method; it crytallizes in the monoclinic system, space group $P2_1/c$ (No.14), with $a = 7.4039(3)$ Å, $b = 7.3838(3)$ Å, $c = 7.4083(3)$ Å, $\beta = 120.36°(1)$, $V = 349.44(2)$ Å^3 and $Z = 4$. The volume of the title compound is comparable to those of the $M^{II}_{0.50}TiO(PO_4)$ series, where M^{II} = Mg, Co, Ni and Zn. The framework is built up from $[TiO_6]$ octahedra and $[PO_4]$ tetrahedra. $[TiO_6]$ octahedra are linked together by corners and form infinite chains along the c-axis. Ti atoms are displaced from the center of octahedral units showing an alternating short distance (1.73 Å) and a long one (2.22 Å). These chains are linked together by $[PO_4]$ tetrahedra. Fe^{2+} cations occupy a triangle-based antiprism sharing two faces with two $[TiO_6]$ octahedra. Mössbauer and magnetic measurements show the existence of iron only in divalent state, located exclusively in octahedral sites with high spin configuration ($t_{2g}^4e_g^2$). Raman study confirms the existence of Ti–O–Ti chains.

Keywords: Synthesis; Oxyphosphate; X-ray diffraction; Magnetic measurements; Mössbauer spectroscopy; Raman spectroscopy

1. Introduction

Inorganic oxyphosphates with the general formula $AMO(XO_4)$ (A = Li, Na, K, Rb, Cs, Tl, Ag; M = Ti, Zr, Sn, Nb, Ta, Sb, X = P, As, Si, Ge have been extensively investigated in the recent years [1–10]. Among these compounds, Ti and K phosphates (or arsenates) constitute an important class of materials that have been intensively studied by numerous structural and spectroscopic methods, as a result of optical properties [11] and other industrial applications. These compounds exhibit a high temperature phase transition from *Pnan* to $Pna2_1$ space group [12–13]. The crystal framework is constructed by three-dimensional chains which are made from corner linked $[TiO_6]$ octahedra and $[PO_4]$ tetrahedra. The short distance in chain between Ti and independent O atom causes a distortion of $[TiO_6]$ octahedra. For instance potassium titanyl phosphate ($KTiO(PO_4)$, or KTP) has been recognized as an outstanding nonlinear optical crystal for electrooptic applications [14]. Nonlinear optic (NLO) crystals, and in particular the KTP single crystal, are commonly used for effective nonlinear transformation of laser radiation, It has a high conversion efficiency for second harmonic generation (SHG), tripling (3HG) and frequency mixing. The qualities and the potential applications of KTP arose great interest in analogs which have partial or complete substitution on K, Ti and P sites. For example McCarron et al. [15] and Peuchert et al. [16] reported on the existence of $K(Mg_{1/3}Nb_{2/3})PO_5$ and $K_2NiWO_2(PO_4)_2$ but the structures are not isostructural with KTP, although their crystal structures are closely related to KTP. On the other hand, K is replaced by small cations leading to new materials in the MO–TiO_2–P_2O_5 system (M = Mg, Co, Ni, Fe, Cu, Zn),

*Corresponding author. Fax: +212 68 55 7819.
E-mail address: s.benmokhtar@univh2m.ac.ma (S. Benmokhtar).

0022-4596/$ - see front matter © 2006 Elsevier Inc. All rights reserved.
doi:10.1016/j.jssc.2006.08.004

such as $Ni_{0.50}TiO(PO_4)$ [17], $Li_{0.50}M_{0.25}TiO(PO_4)$ (M = Ni, Co) [18–20] and $Ni_{(1-x)}Cr_{(1-2x)}Ti_{2x}O(PO_4)$ [21]…which were successfully synthesized, in our laboratory, by several method. In the present paper, we report on the synthesis and the structural characterization, by X-ray diffraction, Mössbauer spectroscopy, magnetic susceptibility and Raman spectroscopy on a new iron oxyphosphate $Fe_{0.50}TiO(PO_4)$.

2. Experimental

2.1. Synthesis

Powder samples of $Fe_{0.50}TiO(PO_4)$ were prepared by solid-state reaction and by exchange reaction.

2.1.1. Solid-state synthesis

Powders of Fe_2O_3, Fe, TiO_2 and TiP_2O_7 are mixed in stoichiometric proportions, according to the scheme:

$$Fe_2O_3 + Fe + 3TiO_2 + 3TiP_2O_7 \rightarrow 6Fe_{0.50}TiO(PO_4).$$

The mixture was placed in a quartz tube and sealed under vacuum, then heated at 650 °C (48 h), 850 °C (48 h) and 1000 °C (36 h) with intermittent regrinding. The X-ray powder diffraction data (XRPD) of the final product shows, in addition to $Fe_{0.50}TiO(PO_4)$, the presence of small amounts of $Fe_{0.5}Ti_2(PO_4)_3$ [22] and TiO_2 rutile (Fig. 1).

2.1.2. Exchange reaction

Since pure phase could not be prepared directly by solid-state reaction, the $Fe_{0.50}TiO(PO_4)$ phase was obtained by ion exchange on two stages.

2.1.2.1.First stage preparation of $Cu_{0.5}TiO(PO_4)$. The preparation procedure was based on the same method as given in Ref. [17]. Stoichiometric amounts of solutions $Cu(NO_3)_2 \cdot 3H_2O$ (I), $(NH_4)H_2PO_4$ (II) and diluted $TiCl_4$ in ethanol (III) as starting materials. The mixture (precipitate + solution), obtained by slow addition of (III) in (I + II) at room temperature, was dried at about 60 °C to remove the volatile compounds. The resultant powder was sequentially heated at 200 °C (4 h), 750 °C (4 h) and 950 °C (6 h) in oxygen atmosphere with intermediate regrinding. This process resulted in a blue compound [23].

2.1.2.2. Second stage preparation of $Fe_{0.50}TiO(PO_4)$. Amounts of metallic iron and $Cu_{0.5}TiO(PO_4)$ in the desired composition ratio were thoroughly homogenized in an agate mortar. Afterwards, this mixture was sealed in quartz tube under vacuum and dried at 900 °C for 5 days according to the reaction

$$Cu_{0.5}TiO(PO_4) + 0.5Fe \rightarrow Fe_{0.50}TiO(PO_4) + 0.5Cu.$$

The XRPD of the resulting product shows the presence of $Fe_{0.50}TiO(PO_4)$ and Cu (Fig. 2). Cu was eliminated by leaching with dilute solution of HNO_3. After filtrating, the sample was washed with distilled water and dried at room temperature. In these conditions a pure iron phase isotype with $Ni_{0.5}TiO(PO_4)$ [17] is obtained. All the characterizations have been done on the sample obtained by exchange reaction.

2.2. Instrumental analysis

The XRPD were collected at room temperature with a Philips PW 3040 (θ-θ) diffractometer using a graphite monochromator.

The structure of the iron oxyphosphate compound was derived from the stepscanned X-ray intensity data, in the range 10–120° (2θ) with a step size of 0.02° (2θ) and counting time of 30 s for each step. The structural

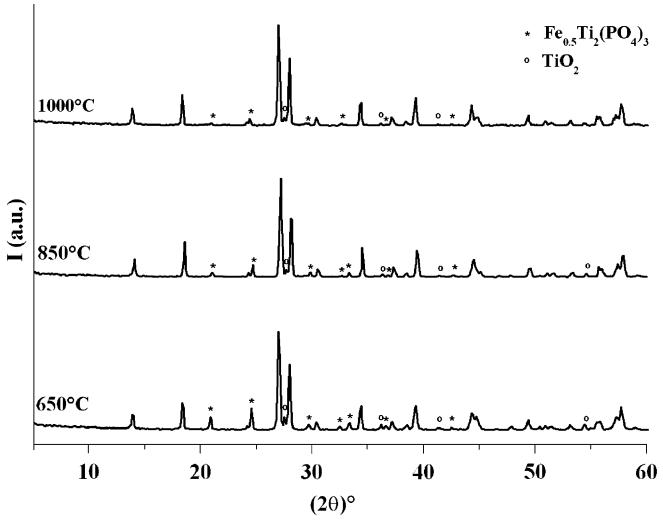

Fig. 1. X-ray powder patterns at room temperature of $Fe_{0.50}TiO(PO_4)$ prepared by solid-state method at various temperatures.

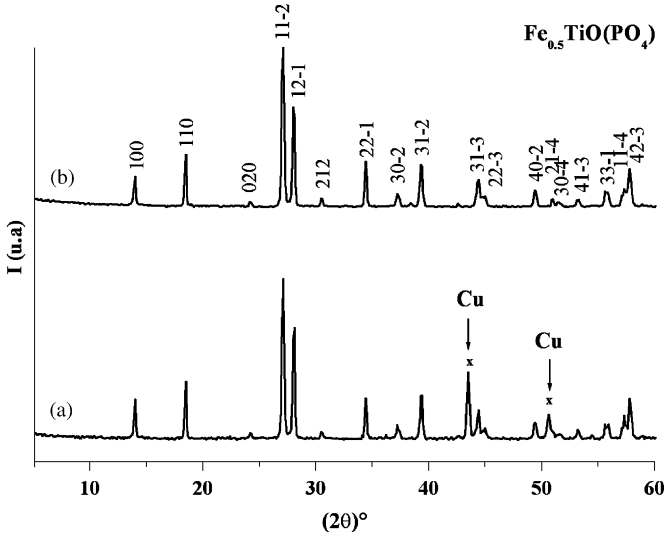

Fig. 2. X-ray powder patterns at room temperature of $Fe_{0.50}TiO(PO_4)$ prepared by exchange reaction at 900 °C, before (a) and after (b) leaching.

parameters were refined by Rietveld method using the computer program FULLPROF [24].

Mössbauer measurements were performed with a constant acceleration HALDER-type spectrometer using a room temperature ^{57}Co source [Rh matrix] in the transmission geometry. Isomer shift values refer to α-Fe at 293 K. The spectra at 4.2 and 293 K were recorded using a variable temperature cryostat.

Magnetic susceptibility measurements were carried out with a Quantum Design SQUID MPMS-5S magnetometer. Data were recorded at a constant applied magnetic field of ($0 < H < 3T$), in the temperature range 4.2–300 K.

The Raman spectra were recorded under the microscope of a Dilor XY Multichannel spectrometer. Excitation was accomplished with the 514.5 nm line of an argon-ion laser. Incident power was approximately 100 mW at the source of which only 10% hit to the sample.

3. Structure determination

The XRPD of $Fe_{0.50}TiO(PO_4)$ was indexed in the monoclinic system with the cell parameters $a = 7.4039(3)$ Å, $b = 7.3838(3)$ Å, $c = 7.4083(3)$ Å and $\beta = 120.36°(1)$ which were comparable with those reported in the literature for similar phases [17,20]. The similarities in the cell parameters of $Fe_{0.50}TiO(PO_4)$ and $Ni_{0.5}TiO(PO_4)$ [17] suggest that the compounds are isostructural. The crystal structure of $Fe_{0.50}TiO(PO_4)$ was derived by Rietveld profile analysis of the X-ray intensity data measured, using the structural parameters of $Ni_{0.5}TiO(PO_4)$ as input data [17] in the monoclinic space group $P2_1/c$ (No. 14). A pseudo-Voigt function was used to describe individual line profiles. The parameters refined include the scale factor, zero point correction, five background parameters, cell parameters, isotropic thermal and positional parameters for all atoms, three coefficients to describe the angular dependence of line breadths and asymmetry factors. In the refinements it should be noted that the displacement parameters for all oxygen atoms were constrained to vary in the same manner. The final indices are $R_P = 0.121$; $R_{WP} = 0.162$; $R_F = 0.0307$; $R_B = 0.0434$, $\chi^2 = 1.95$. In order to confirm our hypothesis of cationic distribution, the Rietveld refinement was reconsidered and 0.5 Ti atom is supposed to occupy the 2*a* site at (0 0 0) position and 0.5 Ti and 0.5 Fe is located at 4*e* site on (~0.73 ~0.22 ~0.53) position [$(Ti_{0.50})_{2a}(Ti_{0.50}Fe_{0.50})_{4e}O(PO_4)$ crystallographic formula]. This last refinement leads to a negative value ($B_{iso(Ti)} = -0.07$ Å^2) for displacement parameters of Ti atom in 2*a* sites. Note that no significant change of the atomic parameters was observed. The best results were therefore obtained for the crystallographic $(Fe_{0.50})_{2a}(Ti)_{4e}O(PO_4)$ formula. The crystal data and details of refinement are given in Table 1. Fig. 3 shows the agreement in the calculated and observed diffraction profiles for $Fe_{0.50}TiO(PO_4)$. The atomic positions and important interatomic distances in the structure of $Fe_{0.50}TiO(PO_4)$ are given in Tables 2 and 3, respectively.

Table 1
Structural data and X-ray Rietveld refinement parameters of $Fe_{0.50}TiO(PO_4)$

Space group	$P2_1/c$
a (Å)	7.4039(3)
b (Å)	7.3838(3)
c (Å)	7.4083(3)
β (deg)	120.366(1)
Volume (Å^3)	349.438(2)
Wavelength (Å)	$\lambda K_{\alpha 1} = 1.54060$; $\lambda K_{\alpha 2} = 1.54442$
Step scan increment (deg 2θ)	0.02
2θ range (deg)	10–120
Program	FULLPROF
Zero point (deg 2θ)	0.0170
Pseudo-voigt function	$\eta = 0.7034(1)$
$[PV = \eta L + (1-\eta)G]$	
Caglioti law parameters	$U = 0.01479(1)$
	$V = 0.00020(9)$
	$W = 0.00246(2)$
No. of reflections	1039
No. of refined parameters	46
R_F	0.0307
R_B	0.0434
R_P	0.121
R_{wp}	0.162
χ^2	1.95

4. Results and discussion

4.1. Description of the structure

The structure of the title compound consists of a three-dimensional (3D) framework built up from [TiO_6] octahedra, one type of Fe polyhedra and isolated [PO_4] tetrahedra (Fig. 4). The [TiO_6] octahedra are linked together in helical chains via bridging O(1); O(1) denote the oxygen atoms which are bonded to the titanium atoms and not implied in [PO_4] tetrahedra. The chains are linked by phosphate tetrahedra parallel to [0 0 1] (Fig. 5). The [TiO_6] are considerably distorted in such a way that titanium atom is displaced from the centre of the octahedron along a Ti–O bond axis, which results in a short bonds (2.92 Å) formed between Ti and Fe.

4.1.1. Titanium atoms

The titanium atoms are coordinated by six oxygen atoms $2O_1$, O_2, O_3, O_4 and O_5, and are displaced from the geometrical centers of the octahedra, resulting in alternating short (1.73 Å) and long (2.22 Å) Ti–O distances with Ti–O and O–O distances ranging, respectively, from 1.73 to 2.22 Å and from 2.66 to 3.98 Å, O–Ti–O angle vary from 76.03 to 168.6 with interoctahedral Ti–O–Ti angles of 140.31° (Fig. 6) this value is close to those found for $LiTiO(PO_4)$ (142.72°) [4] and $Ni_{0.5}TiO(PO_4)$ (139.67°) [17]. The bond lengths distortion parameters Δ of a coordination polyhedron [TiO_6] can be estimated quantitatively using the equation $\Delta = (100/6)\sum_{n=1\ \text{to}\ 6}\{(r_n - \langle r\rangle)/\langle r\rangle\}^2$ %, where r_n and $\langle r\rangle$ are the individual and average

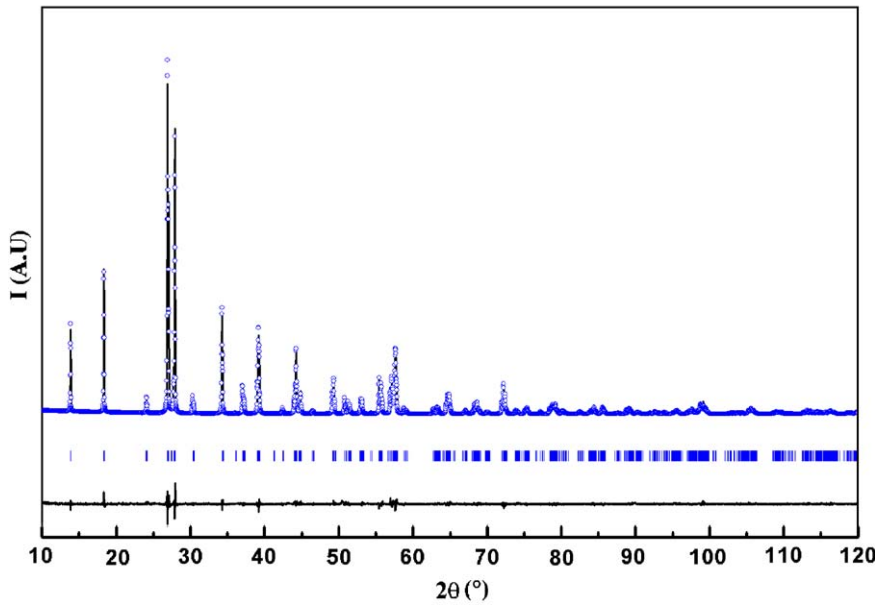

Fig. 3. Final observed (°°°°°), calculated (—) and difference X-ray diffraction patterns for $Fe_{0.50}TiO(PO_4)$.

Table 2
Atomic coordinates and isotropic temperature factors with their estimated standard deviation (ESD)

Atom	Site	x	y	z	B_{iso} (Å^2)	Occ
Fe	2*a*	0.0000	0.0000	0.0000	0.77 (8)	1
Ti	4*e*	0.7341(5)	0.2228(4)	0.5300(4)	0.29 (5)	1
P	4*e*	0.2493(6)	0.1192(5)	0.7498(5)	0.46 (5)	1
O(1)	4*e*	0.7570(12)	0.1600(9)	0.7660(11)	0.47 (8)	1
O(2)	4*e*	0.7773(13)	0.0037(11)	0.0989(14)	0.47	1
O(3)	4*e*	0.4407(11)	0.2405(13)	0.8671(11)	0.47	1
O(4)	4*e*	0.2640(13)	0.0054(11)	0.5887(13)	0.47	1
O(5)	4*e*	0.0625(13)	0.2598(12)	0.1479(13)	0.47	1

bond lengths, respectively [25]. The calculation gives $\Delta = 69$ which is nearly the same as the one determined for $LiTiO(PO_4)$ ($\Delta = 70$) [4] or $Ni_{0.5}TiO(PO_4)$ ($\Delta = 75$) [17] but higher than the value found for TiO_2 (rutile) ($\Delta = 6$) or $M_{0.5}Ti_2(PO_4)_3$ Nasicon type ($M = Mg$, $\Delta = 36$ [26]; $M = Co$, $\Delta = 37$) [27], reflecting the higher instability of Ti^{4+} cations in $M_{0.5}TiO(PO_4)$ oxyphosphates. The difference may be attributed to the strength of O–Ti–O′ bridges connecting the octahedra into infinite chains in the structure of $M_{0.5}TiO(PO_4)$ (Ti–O′ denotes the longer titanium–oxygen distance in the bridge).

4.1.2. Phosphorus atoms

There is one crystallographic site for P^{5+} cations in the $Fe_{0.50}TiO(PO_4)$ structure. The P^{5+} cations are in tetrahedral environment connected to four oxygen atoms with values of bond lengths and bond angles ranging, respectively, from 1.50 to 1.53 Å and from 107.09° to 111.13° as typically in $Ni_{0.5}TiO(PO_4)$ [17] and $LiTiO(PO_4)$ [4]. Each tetrahedron shares two oxygen atoms [O(2) and O(4)] with two [TiO_6] consecutive octahedra of one chain and one oxygen atom O(3) with a neighboring parallel chain.

Table 3
Interatomic distances (Å) and angles (deg) in $Fe_{0.50}TiO(PO_4)$[a]

Ti	O(1)	O(1′)	O(2)	O(3)	O(4)	O(5)
O(1)	*1.73(2)*	168.65(5)	95.07(6)	100.17(6)	102.05(7)	95.32(7)
O(1′)	3.94(3)	*2.22(2)*	76.46(5)	87.54(6)	85.23(5)	76.03(5)
O(2)	2.81(2)	2.66(2)	*2.07(2)*	90.12(6)	160.40(7)	80.69(6)
O(3)	2.78(2)	2.86(3)	2.81(3)	*1.89(2)*	96.08(7)	162.64(9)
O(4)	2.83(3)	2.80(2)	3.91(1)	2.83(1)	*1.90(2)*	88.24(6)
O(5)	2.87(2)	2.68(3)	2.72(5)	3.98(3)	2.81(2)	*2.13(2)*
		⟨Ti–O⟩ = 1.992 (2) Å; V_{sum}(Ti) = 4.1				

Fe	O(1)	O(1′)	O(2)	O(2)	O(5)	O(5)
O(1)	*2.12(1)*	180.0(6)	77.75(5)	102.25(7)	78.08(5)	101.92(6)
O(1′)	4.23(1)	*2.12(1)*	102.25(7)	77.75(5)	101.92(6)	78.08(5)
O(2)	2.66(2)	3.29(3)	*2.12(1)*	180.0(9)	79.38(6)	100.62(7)
O(2)	3.29(3)	2.66(2)	4.22(2)	*2.12(1)*	100.62(7)	79.38(6)
O(5)	2.68(3)	3.31(2)	2.72(5)	3.27(3)	*2.14(1)*	180.0(7)
O(5)	3.31(2)	2.68(3)	3.27(3)	2.71(3)	4.28(2)	*2.14(1)*
		⟨Fe–O⟩ = 2.12 (1) Å; V_{sum}(Fe) = 2.12				

P	O(2)	O(3)	O(4)	O(5)
O(2)	*1.53(2)*	110.97(1.0)	109.70(1.0)	107.21(9)
O(3)	2.52(3)	*1.52(2)*	111.13(9)	107.09(1.0)
O(4)	2.48(3)	2.50(2)	*1.51(2)*	110.67(1.0)
O(5)	2.43(2)	2.42(3)	2.47(3)	*1.50(2)*
	⟨P–O⟩ = 1.517 (2) Å; V_{sum}(P) = 5.05			

[a]The M–O distances are underlined. O–O distances are given below the diagonal and O–M–O angles are given above. The bond valence sum (Vsum) is calculated using the Brown formula: $V_i = \Sigma_j v_{ij} = \Sigma_j \exp[(R_{ij} - d_{ij})/0.37]$ using the parameters d_0, characterizing a cation–anion pair, from reference.

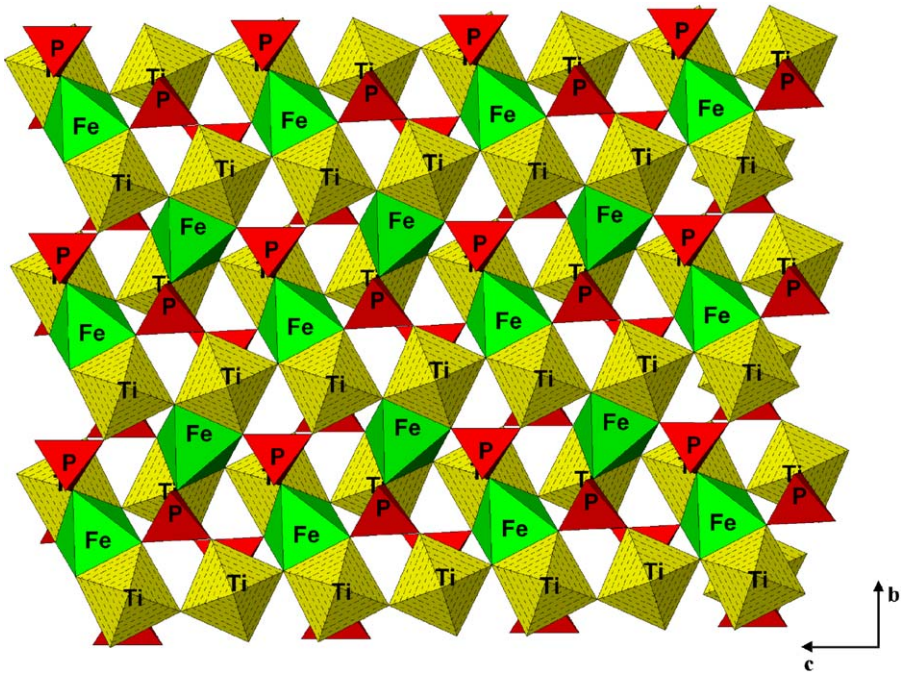

Fig. 4. A polyhedral view of framework as projected in the (b, c) plane.

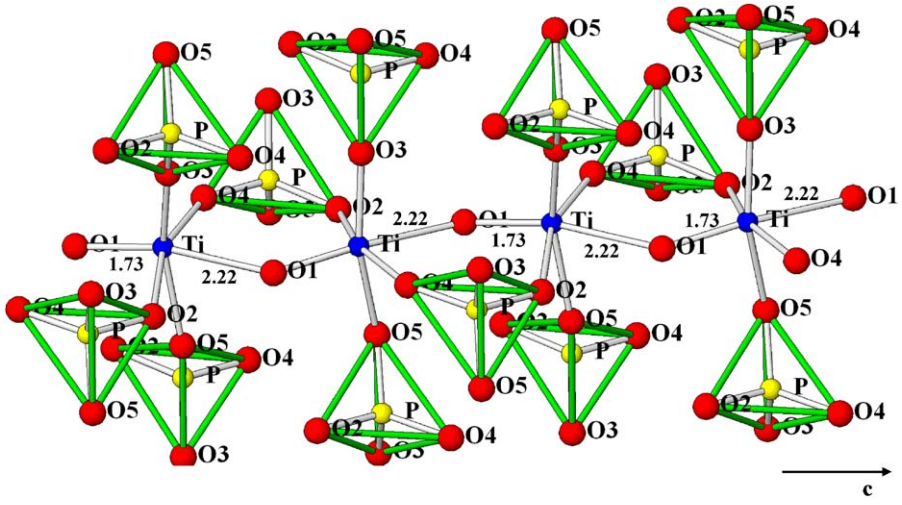

Fig. 5. Chain of TiO_6 octahedra in oxyphosphate $Fe_{0.50}TiO(PO_4)$ linked to PO_4 tetrahedra, along *c*-axis.

4.1.3. Iron atoms

Iron cations are located in the cavities of the structure, this cation surrounded by six oxygen atoms $2O_1$, $2O_2$ and $2O_5$ forming an octahedral site. As will be shown below, ^{57}Fe Mössbauer spectroscopy can be used as a definite proof for this assignment, but also the bond valence sum [28–29] at the Fe-site with 2.12 valence units gives a hint that the site is occupied by Fe^{2+} only. The Fe–O bond lengths range between 2.12(1) and 2.14(1) Å are practically equal to the ionic radii sum of O^{2-} and Fe^{2+} (2.12 Å) [25]. The $[FeO_6]$ octahedra are isolated from each other and the Fe^{2+}–Fe^{2+} distance is 5.22 Å. Every octahedron shares two faces with two $[TiO_6]$ groups and four corners with $[PO_4]$ tetrahedra (Fig. 7).

4.1.4. Bond valence sum

The correctness of the structure was confirmed by bond-valence calculations from the Brown method $V_i = \sum_j v_{ij}$ and $v_{ij} = \exp[(R_{ij} - d_{ij})/0.37]$, using the parameters R_{ij}, characterizing a cation–anion pair (O^{2-}: 1.815 Å for Ti^{4+}, 1.734 Å for Fe^{2+} and 1.604 Å for P^{5+}) [28–29], d_{ij} the distance between *i* and *j* atoms. The results are in good agreement with the theoretical values for the expected formal oxidation state of Ti^{4+}, P^{5+}, Fe^{2+} and O^{2-} ions (Table 4).

4.2. Magnetic susceptibility

The thermal variation of the reciprocal magnetic susceptibility (Fig. 8) between 4 and 300 K show almost linear behavior and can be fitted by the simple Curie–Weiss equation $\chi(T) = C/(T-\theta)$, where $C = 3.29$ is the Curie constant and $\theta_p = (-2 \pm 1)K$ is the Weiss constant. The low negative Weiss constant implies low antiferromagnetic interactions between Fe^{2+} ions, in good agreement with structural data which showed that Fe^{2+} ions are located in isolated oxygen antiprisms with large Fe–Fe distances ($dFe^{2+}-Fe^{2+} = 5.22$ Å). The effective magnetic moment ($\mu_{eff} = (8C)^{1/2}$) was calculated to be 5.13 μB per Fe^{2+} ion. This value is typical for the oxidation state (+II) of iron in octahedral sites with high spin configuration (Fe^{2+}: $t_{2g}^4 e_g^2$) [30].

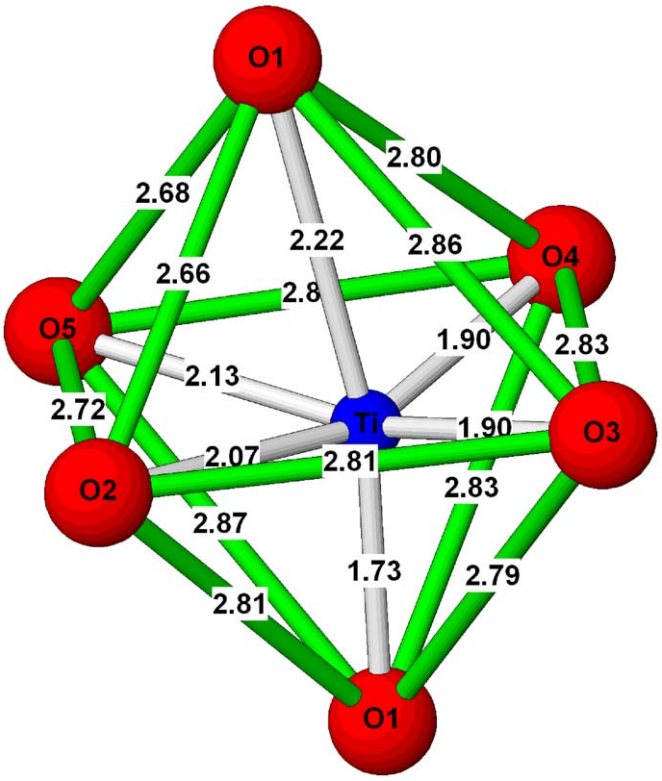

Fig. 6. The titanium atom in sixfold coordination.

4.3. Mössbauer spectroscopy

The ^{57}Fe Mössbauer spectra of $Fe_{0.50}TiO(PO_4)$, recorded at 293and 4.2 K, are shown in Fig. 9. The points represent experimental results, and the continuous line corresponding to computer fitted data. A preliminary refinement using Lorentzian profile lines show that the spectra consists of two fine peaks, one doublet assigned only to Fe^{2+} ions. The hyperfine parameters obtained from this refinement

Table 4
Bond valence calculation for $Fe_{0.50}TiO(PO_4)$

	Fe	Ti	P	V_i	$V_{théo}$
O(1)	0.362 (× 2)	1.225		1.922	2
O(1′)		0.335			
O(2)	0.362 (× 2)	0.502	1.221	2.085	2
O(3)		0.816	1.255	2.071	2
O(4)		0.795	1.289	2.084	2
O(5)	0.334 (× 2)	0.427	1.289	2.05	2
V_i	2.116	4.1	5.054		
V_{theo}	2	4	5		

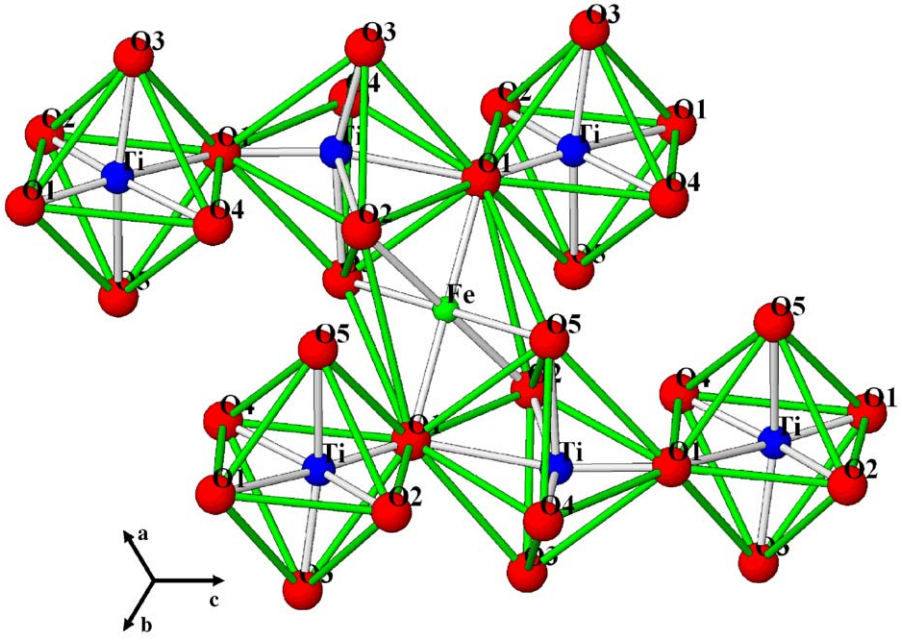

Fig. 7. The polyhedral environments around the [TiO_6] and [FeO_6] octahedra in oxyphosphate $Fe_{0.50}TiO(PO_4)$.

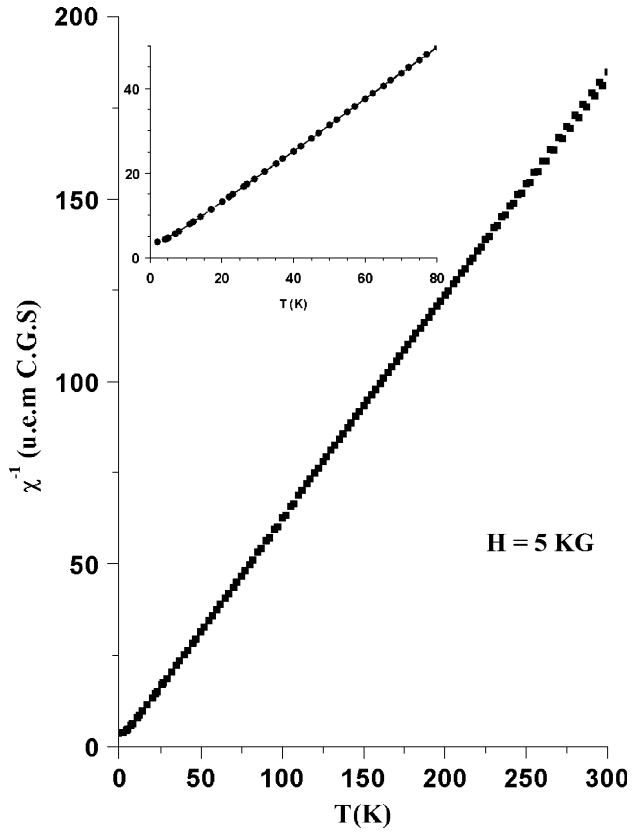

Fig. 8. Reciprocal molar magnetic susceptibility of $Fe_{0.50}TiO(PO_4)$ as a function of temperature.

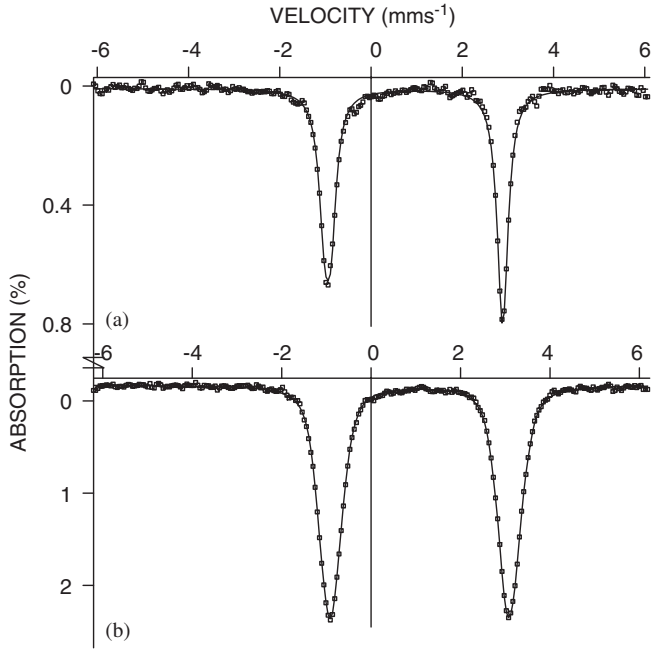

Fig. 9. Mössbauer spectra of $Fe_{0.50}TiO(PO_4)$ (a) $T = 293\,K$, (b) $T = 4.2\,K$.

are given in Table 5. The values of isomer shift (δ), quadruple splitting (Δ) and width at half-maximum (Γ) are typical of high spin Fe^{2+} ions in an octahedral oxygen environment [31,32]. These results are in accordance with magnetic results and structural refinement, which indicted the presence of a Fe^{2+} in one site with octahedral environments.

Table 5
Mössbauer parameters of $Fe_{0.50}TiO(PO4)$

Compound	T (K)	$\delta \pm 0.01$ (mm s^{-1})	$\Delta \pm 0.01$ (mm s^{-1})	$\Gamma_2 \pm 0.01$ (mm s^{-1})	$\Gamma_1 \pm 0.01$ (mm s^{-1})
$Fe_{0.50}TiO(PO_4)$	293	1.11	3.85	0.28	0.38
	4.2	1.24	4.02	0.30	0.30

Table 6
Correlation scheme for$(PO_4)^{3-}$ tetrahedra in $Fe_{0.50}TiO(PO_4)$

T_d	C_1	C_{2h}: factor group
A_1	A	Ag + Bg + Au + Bu
E	2A	2Ag + 2Bg + 2Au + 2Bu
T_2, F_2	3A	3Ag + 3Bg + 3Au + 3Bu

4.4. Raman spectroscopy

4.4.1. P–O bonds

The tetrahedral $(PO_4)^{3-}$ free ion with T_d symmetry has four internal modes of vibration [33], symmetric and antisymmetric stretching modes ($\nu_1(A_1) = 938\,cm^{-1}$, $\nu_3(F_2) = 1017\,cm^{-1}$) and bending modes ($\nu_2(E) = 420\,cm^{-1}$, and $\nu_4(F_2) = 567\,cm^{-1}$) of which $\nu_1(A_1)$ and $\nu_2(E)$ are Raman active modes , $\nu_3(F_2)$ and $\nu_4(F_2)$ are both IR and Raman active modes. With theoretical group analysis method [34], we carried out the number of the vibrations and determine the IR and Raman active modes. Table 6 gives the correlation scheme for the stretching modes of $(PO_4)^{3-}$ groups through the site symmetry in the title compound.

In $Fe_{0.50}TiO(PO_4)$ ($P2_1/c$ space group) the phosphorous atom is in a C_1 symmetry site; therefore, we expect eight Raman-active modes for the stretching vibrations; $\nu_1(PO_4)$ (Ag + Bg) + $\nu_3(PO_4)$ (3Ag + 3Bg). For the bending vibrations 10 Raman-active modes; $\nu_2(PO_4)$ (2Ag + 2Bg) + $\nu_4(PO_4)$ (3Ag + 3Bg) are predicted. The external modes consist of the translational vibrations of the Ti^{4+}, Fe^{2+} and PO_4^{3-} ions and PO_4^{3-} librations [35–36].

Raman spectrum of the oxyphosphate $Fe_{0.50}TiO(PO_4)$ is plotted in Fig. 10. Generally, for phosphates the antisymmetric stretching modes are found between 1290 and 1050 cm^{-1} and the symmetric stretching modes lay between 1050 and 900 cm^{-1} (Table 7). The P–O assignments of the oxyphosphate $Fe_{0.50}TiO(PO_4)$ is in good agreement with those found on $KTiO(PO_4)$, $NaTiO(PO_4)$, $LiTiO(PO_4)$ and $Ni_{0.5}TiO(PO_4)$ oxyphosphates [37–39] exhibiting a structure close to that of $Fe_{0.50}TiO(PO_4)$ and the same type of P–O bonds. Such P–O bonds are also found in the compound $KTiO(PO_4)$ studied by Bushiri [37].

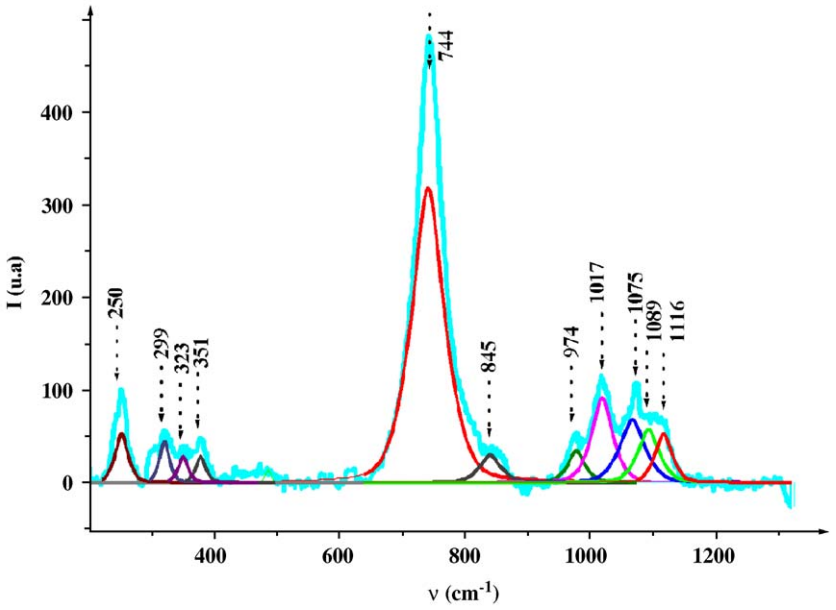

Fig. 10. Raman spectrum of oxyphosphate $Fe_{0.50}TiO(PO_4)$.

Table 7
Description of the chemical bonds in the oxyphosphates

Compounds	Type	Short length (Å)	$\nu_{MO6}(cm^{-1})$	Ref
$Fe_{0.50}TiO(PO_4)$	Ti–O–Ti	1.73	744	[This work]
$Ni_{0.5}TiOPO_4$	Ti–O–Ti	1.70	750	[39]
$LiTiOPO_4$	Ti–O–Ti	1.70	783	[39]
$NaTiOPO_4$	Ti–O–Ti	1.70	745	[38]
$KTiOPO_4$	Ti–O–Ti	1.72	698	[37]
$Na_4TiO(PO_4)_2$	Ti–O–Ti	1.93	687	[38]
$(TiO)_2P_2O_7$	Ti–O–Ti	1.76	719	[40]
$SbO(PO_4)$	Sb–O–Sb	1.90	780	[41]

Table 8
Raman bands and empirical assignments for the oxyphosphate $Fe_{0.50}TiO(PO_4)$

Assignments	Bands (cm^{-1})	
$\nu_3(T_2)$	1116, 1089, 1075	vas and vs (P–O) stretching modes
$\nu_1(A_1)$	1017, 974, 845	
ν_{TiO6}	744	Symmetric stretching mode Ti–O
$\nu_4(T_2)$	491, 471	δ(O–P–O) deformation modes
$\nu_2(E)$	351	
Translational vibrations of the Ti^{4+}, Fe^{2+} and PO_4^{3-} ions and PO_4^{3-} librations	323, 299, 250	

4.4.2. Ti–O bonds

The Ti–O(1)–Ti bonds created by corner-shared linkage of octahedra have a short length of 1.73 Å. The stretching frequency is found at 744 cm^{-1}. The assignment was made on the basis of previous literature results for oxyphosphates with infinite chains (Table 8). The high value of the frequency Ti–O can be explained by the short length of Ti–O bond existing in the $[TiO_6]$ octahedral chains, which allows the couplings of the Ti–O vibrations in these chains.

5. Conclusions

In the present work, a new phosphate $Fe_{0.50}TiO(PO_4)$ has been synthesized by Cu^{2+}–Fe^{2+} ion exchange reaction. Structure of this new phosphate has been refined from X-ray powder diffraction using Rietveld method. The new phosphate belongs to the oxyphosphate family $M_{0.5}TiO(PO_4)$ (M = Mg, Fe, Co, Ni, Zn, etc.) and crystallizes in the $P2_1/c$ space group. The structure is formed by a 3D network of $[TiO_6]$ octahedra and $[PO_4]$ tetrahedra where octahedral cavities are occupied by iron atoms. $[TiO_6]$ octahedra are linked together by corners and form infinite chains along c-axis. Ti atoms are displaced from the center of octahedral units showing an alternating short distance (1.73 Å) and a long one (2.22 Å). Powder of the oxyphosphate $Fe_{0.50}TiO(PO_4)$ was characterised by Mössbauer and Raman spectroscopies and by magnetic measurements. Results are in good agreement with structural data.

Acknowledgments

We would like to thank the ICMCB-CNRS France, especially O. Viraphong for useful discussions and technical assistance during the experiment and Eric Lebraud, S. Péchev for help during the data collection. Bouchaib Manoun for assistance in obtaining the Raman spectra (Post doc Department of Chemistry, University of Pretoria South Africa).

References

[1] F.Z. Zumsteg, J.D. Bierlein, T.E. Gier, J. Appl. Phys. 47 (1976) 4980.
[2] J. Alexander Speer, G.V. Gibbs, Am. Mineral. 61 (1976) 238.
[3] H. Nyman, M. O'Keeffe, Acta Crystallogr. B 34 (1978) 905.
[4] P.G. Nagornoy, A.A. Kapshuck, N.V. Stuss, N.S. Slobodyanik, Zh. Neorg. Khim. 34 (1989) 3030.
[5] M.L.F. Phillips, W.T.A. Harrison, G.D. Stucky, Inorg. Chem. 39 (1990) 3245.
[6] A. Robertson, J.G. Fletcher, J.M.S. Skakle, A.R. West, J. Solid State Chem. 109 (1994) 53.
[7] M. Kunz, R. Dinnebier, L.K. Cheng, E.M. McCarron, D.E. Cox, J.B. Parise, M. Gehrke, J.C. Calabresse, P.W. Stephens, T. Vogt, R. Papoular, J. Solid State Chem. 20 (2) (1995) 299.
[8] W.T.A. Harrison, T.E. Gier, G.D. Stucky, A.J. Schultz, Mater. Res. Bull. 30 (11) (1999) 1341.
[9] S.T. Norberg, J. Gustafsson, B.E. Mellander, Acta Crystallogr. B 59 (2003) 588.
[10] M. Simpson, W.T.A. Harrison, Solid State Sciences 6 (2004) 981.
[11] I. Tordjman, R. Masse, J.C. Guitel, Z. Kristallogr. 139 (1974) 103.
[12] W.T.A. Harrison, T.E. Gier, G.D. Stucky, A.J. Schultz, Mater. Res. Bull. 30 (1995) 1341.
[13] P. Delarue, C. Lecomte, M. Jannin, G. Marnier, B. Menaert, Phys. Rev. B 58 (1998) 5287.
[14] G.D. Stucky, M.L.F. Phillips, T.E. Gier, Chem. Mater. 1 (1989) 492.
[15] E.M. McCarron III, J.C. Calabrese, T.E. Gier, L.K. Cheng, C.M. Foris, J.D. Bierlein, J. Solid State Chem. 102 (1993) 354.
[16] U. Peuchert, L. Bohaty, J. Schreuer, Acta Crystallogr. C 53 (1997) 11.
[17] P. Gravereau, J.P. Chaminade, B. Manoun, S. Krimi, A. El Jazouli, Powder Diffr. 14 (1999) 10.
[18] B. Manoun, A. El Jazouli, P. Gravereau, J.P. Chaminade, F. Bouree, Powder Diffr. 17 (4) (2002) 290.
[19] B. Manoun, A. El Jazouli, P. Gravereau, J.P. Chaminade, Mater. Res. Bull. 40 (2005) 229.
[20] A. El Jazouli, H. Belmal, S. Krimi, B. Manoun, J.P. Chaminade, P. Gravereau, D. De Waal,. Proceding of the 12th International Conference on Solid Compound of Transition Elements Saint Malo, 1997.
[21] B. Manoun, A. El Jazouli, P. Gravereau, J.P. Chaminade, J.C. Grenier, Ann. Chim. Sci. Mater. 25 (Suppl. 1) (2000) 71.
[22] !S. Benmokhtar, A. El Jazouli, J.P. Chaminade, P. Gravereau, A. Wattiaux, L. Fournes, J.C. Grenier, Phosphorus Res. Bull. 15 (2003) 127.
[23] P. Gravereau, S. Benmokhtar, J.P. Chaminade, A. El Jazouli, E. Lebraud, S. Péchev, Proceeding of the XX Congress of the International Union of Crystallography, Florence, 23–31 August 2005.
[24] J. Rodriguez-Carvajal, Collected Abstract of Powder Diffraction Meeting, Toulouse, France, 1990, 127.
[25] R.D. Shannon, Acta Crystallogr. A 32 (1976) 751.
[26] S. Barth, R. Olazcuaga, P. Gravereau, G. Le Flem, P. Hagenmuller, Mater. Lett. 16 (1993) 96.
[27] R. Olazcuaga, J.M. Dance, G. Le Flem, J. Derouet, L. Beaury, P. Porcher, A. EL Bouari, A. El Jazouli, J. Solid State Chem. 143 (1999) 224.
[28] I.D. Brown, D. Altermatt, Acta Crystallogr. B 41 (4) (1985) 244.
[29] N.E. Brese, M. O'Keeffe, Acta Crystallogr. B: Struct. Sci. 47 (1991) 192.
[30] C. Kittel, Introduction to Solid State Physics, sixth ed, Wiley, New York, 1986 p406.
[31] N.N. Greenwood, T.C. Gibb, Mössbauer Spectroscopy, Chapman & Hall, London, 1971 p659.
[32] C. Gleitzer, Eur. J. Solid State Inorg. Chem. 28 (1991) 77.
[33] A. Müller, B. Krebs, J. Mol. Spectrosc. 24 (1967) 180.
[34] F.A. Cotton, Chemical Applications of Group theory, Wiley Interscience, NY, 1971.
[35] K. Nakamoto, third ed, Wiley-Interscience, New York, 1977, p. 142.
[36] D.M. Adams, D.C. Newton, Beckmann, Croydon, 1970.
[37] M.J. Bushiri, V.P. Mahadevan Pillai, R. Ratheesh, V.U. Nayar, J. Phys. Chem. Solids 60 (1999) 1983.
[38] C.E. Bamberger, G.M. Begun, O.B. Cavin, J. Solid. State Chem. 73 (1988) 317.
[39] A. El Jazouli, S. Krimi, B. Manoun, J.P. Chaminade, P. Gravereau, D. De Waal, Ann Chim. Sci. Mat. 23 (1998) 7.
[40] C.E. Bamberger, G.M. Begun, J. Less-common Metals 134 (2) (1987) 201.
[41] E. Husson, F. Genet, A. Lachgar, Y. Piffard, J. Solid State Chem. 75 (1988) 305.